


CHEMOSTRATIGRAPHIC ARCHITECTURE OF SANDSTONE FACIES EXPOSED ALONG AUCHI-IGHARA ROAD, MID-WESTERN NIGERIA

Phillips Reuben IKHANE¹ , Odunayo Christy ATEWOLARA-ODULE² , Olalekan Olayiwola OYEBOLU¹ ,
Omotoso Richard FAKOLADE³ 

1 Olabisi Onabanjo University, Department of Earth Sciences, Ago-Iwoye, Ogun State

2 Olabisi Onabanjo University, Department of Chemical Science, Ago-Iwoye, Ogun State

3 Federal Polytechnic, Department of Mineral Science, Ado-Ekiti, Ekiti State

E-mail: phillipsikhane@gmail.com

ABSTRACT

In this work, inorganic whole-rock geochemistry was applied to characterize the exposed sandstone facies along the Auchu-Ighara road Anambra basin Midwestern, Nigeria for distinction and correlation of the depositional units on the basis of the stratigraphic variation of geochemical trait. Fourteen representative samples collected from the outcrop were analyzed using Inductively Coupled Plasma-Mass Spectrometer (ICP-MS). From our analyses, ten major elements oxides, sixteen trace elements, and thirteen rare earth elements were obtained. The concentration of major elements in the samples range from 0.13 % and 53.71 % with SiO₂, TiO₂, Al₂O₃ and Fe₂O₃ being predominant. Other oxides found in the samples include K₂O, CaO, Na₂O, MgO and P₂O₅ indicating a recycled orogenic source of the grits from which the sandstone is derived. Trace elements concentration ranges between 0.017 ppm and 122.25 ppm; marked by the dominance of Zircon (Zr) which further asseverates orogenic recycling. The rare earth elements range in concentration from 0.01ppm and 5.53 ppm; the modal occurrence of Praseodymium (Pr) in this category is apparently indicative of deposition in an oxidizing environment. The appreciably high SiO₂/Al₂O₃ ratio averages 11.2 in the samples is symptomatic of several cycles of sedimentation. Variation pattern of Ga/Rb and Al₂O₃/(CaO+MgO+K₂O+Na₂O) ratios connote a cooler and drier climatic condition after the sandstone deposition, which expectedly resulted to a decrease in hydrolytic weathering. Changes in sediment provenance are predicated on Cr/Al₂O₃, Cr/Na₂O and Nb/Al₂O₃ ratio which indicate grits derivation from a more quartzose sedimentary and felsic sources that resulted from fluctuating paleoclimate during deposition. From the geochemical data, the paleoclimate and provenance of the sandstone facies were modelled and used for subdivision and correlation into two geochemical packages and five geochemical units.

Keywords: Chemostratigraphy; Paleoclimate; Provenance; Weathering; Whole rock geochemistry.

1 INTRODUCTION

The application of geochemical proxies now transcends their original usage for paleo-environmental reconstruction because chemical signature or fingerprints of sedimentary sequence when interrelated are viable tool for stratigraphic correlation. The fact that sedimentary rocks are faithful recorders of the changes in provenance, environment of deposition and post-depositional history cannot be overemphasized. The implication of such changes is that apparently uniform sediment successions can display primary differences in the constituent minerals chemistry as well as the proportionate accessory phases of clays and heavy minerals many of which may show distinct chemical composition [1]. As these subtle changes produce different combinations of minerals, there are distinctive major and trace elemental composition of the sediments that can be utilized to characterize and correlate the ensuing rocks [2].

Chemostratigraphy therefore seeks the application of the major and trace element geochemistry or fingerprints for the characterisation and subdivision of sedimentary sequences into geochemically distinct units as well as

correlating strata. This approach was applied in this work to characterize the rocks, and to correlate the lithostratigraphic units based on inorganic geochemical affinities.

2 GEOLOGICAL SETTINGS OF THE STUDY AREA

The study area falls within longitude $6^{\circ}13'19.4''$ – $6^{\circ}14'01''$ E and latitude $7^{\circ}17'46''$ – $7^{\circ}18'19.3''$ N along an easily accessible Auchi-Igarra road (Fig. 1) and is located in the western Benin side of Anambra basin.

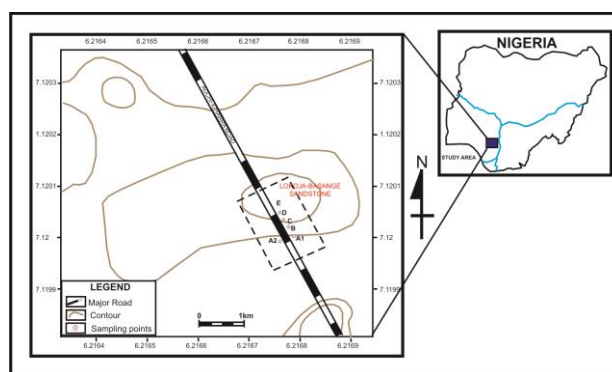


Figure 1. Location map of the study

The separation of the South American and African lithospheric plates in the Mesozoic era led to various tectonic activities which resulted in the formation of several sedimentary basins (Fig. 2) in Nigeria [3]. The Anambra basin became an active depocentre after the Santonian orogeny [4], accommodating appreciable thickness of the Pre-Santonian sediments which covers the basement as confirmed by gravity studies. The basin is subdivided into two sub-basins (i.e., western Benin flank and the eastern Calabar flank) by the “Nsukka High” [4]. The depositional style in the basin exhibits a progressive deepening of sediment from lower coastal plain and shoreline deltas to the shoreline and shallow marine deposits [5]. The stratigraphy column of Anambra basin is briefly explained in Table 1.

The exposed sedimentary sequence in the study area falls within Lokoja-Bassange formation, on the Benin flank of Anambra basin. It is laterally equivalent to the graded Bawa sandstones, and underlain by Precambrian basement rocks [6].

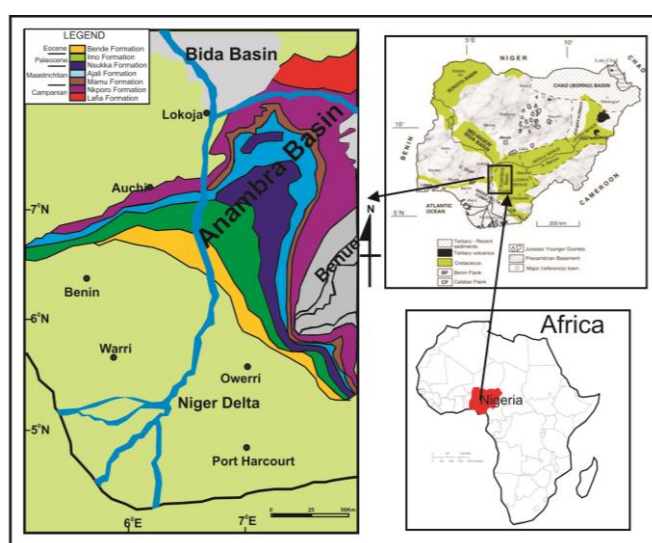


Figure 2. Geological provinces of Nigeria (modified from [3])

Table 1. Lithostratigraphy of Anambra basin (modified from [7] and [8])

AGE	SEDIMENTARY SEQUENCE	LITHOLOGY	DESCRIPTION	DEPOSITIONAL ENVIRONMENT	REMARKS		
					Coal Rank	ANKPA SUB-BASIN	ONITSHA SUB-BASIN
MIOCENE	OGWASHI-ASABA FM.		Lignites, peats, intercalation of Sandstones & shales	Estuarine (off shore bars, intertidal flats)	Liginites		REGRESSION
OLIGOCENE							
EOCENE	AMEKE FM. / NANKA SAND		Clays shales, sandstones & beds of grits	Subtidal intertidal flats, shallow marine	Unconformity		(Continued Transgression Due to geoidal Sea level rise)
PALEOCENE	IMO SHALE		Clays, shales & siltstones	Marine			
MAASTRICHTIAN	NSUKKA FM.		Clays, shales, thin sandstones & coal seams	Estuarine	Sub-bituminous		TRANSGRESSION (Geoidal sea level Rise plus crustal Movement)
	AJALI SST.		Coarse sandstones, Lenticular shales, beds of grits & Pebbles	Subtidal, shallow marine			
	MAMU FM.		Clays, shales, carbonaceous shale, sandy shale & coal seams	Estuarine/off-shore bars/tidal flats/ chernier ridges	Sub-bituminous		
CAMPANIAN	ENUGU/ NKPORO SHALE		Clays & shales	Marine	3rd Marine cycle		
CONIACIAN-SANTONIAN	AWGU SHALE		Clays & shales	Marine	2nd Marine cycle		
TURONIAN	EZEAKU SHALE				1st Marine cycle		
CENOMANIAN	ODUKPANI FM.				Unconformity		
ALBIAN	ASU RIVER GP.				Unconformity		
L. PALEOZOIC	B A S E M E N T C O M P L E X				Unconformity		

3 MATERIAL AND METHODS

Fourteen fresh representative samples were carefully collected from the outcrop of the sandstone facies (Fig. 3). Analysis of these samples was accomplished through Inductively Coupled Plasma-Mass spectrometric (ICP-MS) technique, using lithium metaborate/ tetra-borate fusion to obtain the inorganic geochemical analytical results for the major, trace and rare earth elements contained in the samples out of which only relatively small number would be used for chemostratigraphic characterization of the area [9] and [10].

Facies change examination in the study was based on the work of [11] which states that whole rock geochemistry variations occur along lithologic boundaries in any siliciclastic sequence. Authors in [12] further asseverate that chemical classification of siliciclastic rocks can be achieved based on the ratios of certain oxides and key elements, known as lithologic ratios. Oxides employed for this classification were SiO₂, Al₂O₃, MgO and Fe₂O₃; and SiO₂/Al₂O₃ lithologic ratio (Table 2).

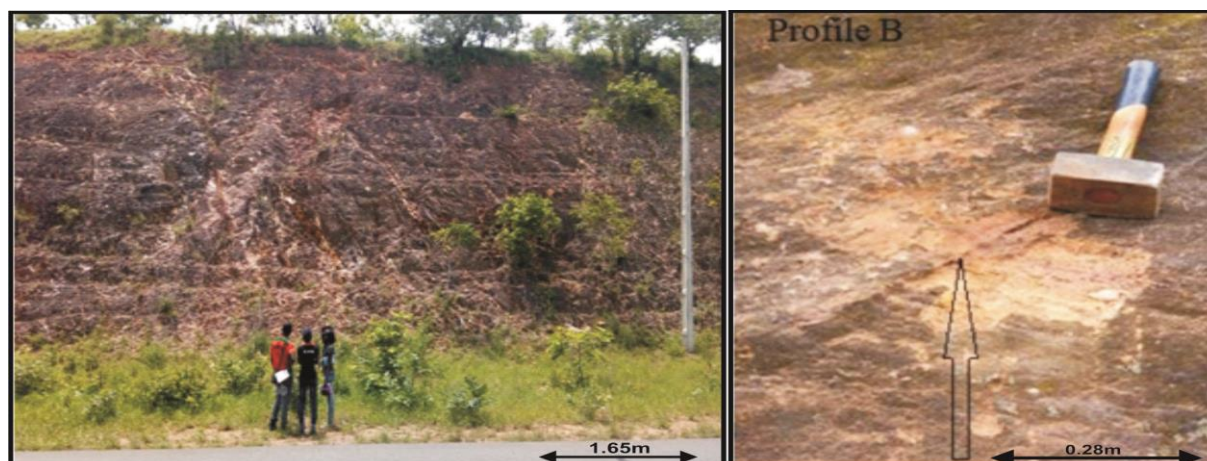


Figure 3. Exposed sandstone facies along Auchi-Igarra road

Table 2. Lithologic ratios used for siliciclastic rocks classification (modified from [12])

Siliciclastic lithologies	
Silty Claystone/Claystone	$\text{SiO}_2/\text{Al}_2\text{O}_3 < 4$
Siltstones	$\text{SiO}_2/\text{Al}_2\text{O}_3 = 4-6$
Argillaceous sandstone	$\text{SiO}_2/\text{Al}_2\text{O}_3 = 6-10$
Sandstone	$\text{SiO}_2/\text{Al}_2\text{O}_3 * 10$
Dolomitic sandstone	*MgO 5% & $\text{SiO}_2/\text{Al}_2\text{O}_3 * 10$
Ferruginized lithologies	
$\text{SiO}_2/\text{Al}_2\text{O}_3 < 4$	*10% Fe_2O_3 Fe-rich Silty claystone
$\text{SiO}_2/\text{Al}_2\text{O}_3 = 4-6$	Fe-rich Siltstone
$\text{SiO}_2/\text{Al}_2\text{O}_3 = 6-10$	Fe-rich Argillaceous Sandstone
$\text{SiO}_2/\text{Al}_2\text{O}_3 * 10$	Fe-rich Sandstone

The ratio of stable to mobile elements in the sample was interpreted for the prediction of hydrologic weathering rate [13]. $\text{Al}_2\text{O}_3/\text{SiO}_2$ ratio in siliciclastic rocks is a viable tool for delineating the degree of quartz enrichment and weathering rate [14]. Gallium (Ga) and Rubidium (Rb) are both controlled by clay mineral distribution; however, Ga is commonly in kaolinite [15], whereas Rb is more prevalent in illite, where it replaces K_2O [16]; thus, (Ga/Rb) ratio can be used to reflect the kaolinite/illite ratio in any given sample. Also, the formation of kaolinite and illite typically occur under humid tropical and drier cooler climate respectively. Therefore, an essential plot for paleo-climate prediction in this research combined the use of Ga/Rb ratio and $\text{Al}_2\text{O}_3/\text{bases}$. In addition, the ratio of the relatively immobile Thorium (Th) and Uranium (U) was used to evaluate the degree of rock weathering. In most upper continental rocks, the ratio is typically between 3.5 and 4.0 [17]. In sedimentary rocks, Th/U values higher than 4.0 may indicate intense weathering in the source areas or sedimentary recycling. Also, the relationship between Th/U ratio and Th concentration was additionally applied to further ascertain weathering rate of the investigated samples [17].

Zircon (Zr) and Titanium oxide (TiO_2) were both related principally to silt-grade heavy minerals, Zr being associated with Zircons and TiO_2 with Ti-oxides such as Rutile and Anatase [18]. The Na_2O value was used as probable index of the plagioclase feldspar content in the sandstone samples.

3.1 Provenance signatures

The discriminant function diagram proposed by [19] was adopted to unravel the provenance of the Lokoja-Bassange formation. These authors noted that biogenic CaO and SiO_2 in provenance determination could be eliminated by a plot in which the discriminant functions are based upon the ratios of individual TiO_2 , Fe_2O_3 , MgO and K_2O to Al_2O_3 which is more reliable and effective than the one based upon the raw oxides. Accordingly, the discriminant plots used in this study include:

$$\text{Discriminant Function (DF1)} = -1.773\text{TiO}_2 + 0.607\text{Al}_2\text{O}_3 + 0.76\text{Fe}_2\text{O}_3(T) - 1.5\text{MgO} + 0.616\text{CaO} + 0.509\text{Na}_2\text{O} - 1.224\text{K}_2\text{O} - 9.09$$

$$\text{Discriminant Function (DF2)} = 0.445\text{TiO}_2 + 0.07\text{Al}_2\text{O}_3 - 0.25\text{Fe}_2\text{O}_3(T) - 1.42\text{MgO} + 0.438\text{CaO} + 1.475\text{Na}_2\text{O} + 1.426\text{K}_2\text{O} - 6.861$$

Delineation of the tectonic setting of the study area also involved the use of discriminant bivariate plot of first and second discriminant functions of major element analysis of the sample. The discriminant functions for tectonic setting determination [14] are as follows:

$$\text{Discriminant function 1} = -0.0447\text{SiO}_2 - 0.972\text{TiO}_2 + 0.008\text{Al}_2\text{O}_3 - 0.267\text{Fe}_2\text{O}_3 + 0.208\text{FeO} - 3.082\text{MnO} + 0.140\text{MgO} + 0.195\text{CaO} + 0.719\text{Na}_2\text{O} - 0.032\text{K}_2\text{O} + 7.510\text{P}_2\text{O}_5 + 0.303$$

$$\text{Discriminant function 2} = -0.421\text{SiO}_2 + 1.988\text{TiO}_2 - 0.526\text{Al}_2\text{O}_3 - 0.551\text{Fe}_2\text{O}_3 - 1.610\text{FeO} + 2.720\text{MnO} - 0.907\text{CaO} - 0.177\text{Na}_2\text{O} - 1.840\text{K}_2\text{O} + 7.244\text{P}_2\text{O}_5 + 43.57$$

4 RESULTS

4.1 Lithologic description

The exposed outcrop is about 20m thick sedimentary sequence and consists of coarse-grained sandstones intercalated with clayey materials at the top of the section (Fig. 4). Light brownish-whitish-yellowish-pale-brownish medium to coarse textured, moderately sorted sandstone predominates the mid-section, with the observed colour variation attributable to composition differences of the cementing material binding the clasts; while the basal unit distinguishably consists of prominent brownish medium to coarse grained, moderately sorted sandstones cross laminated with kaolinitic materials (Fig. 4).

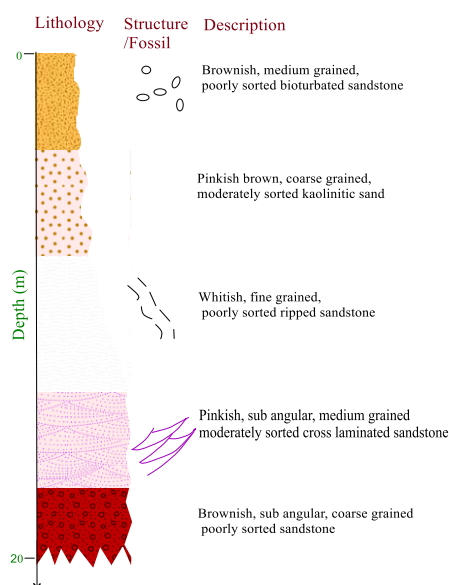


Figure 4. Lithologic section of the sandstone outcrop

4.2 Compositional analysis

Spectrometric result of the analyzed samples revealed disproportionate occurrence of 10 major oxides, namely; SiO_2 , A_2O_3 , Fe_2O_3 , MgO , Na_2O , TiO_2 , K_2O , MnO , P_2O and CrO_3 (Fig. 5a); 16 trace elements which are Be, Co, Cs, Ca, Hf, Th, Nb, Rb, Sn, Sr, Ta, U, W, Zr, and Ga (Fig. 5b); and 13 rare earth elements viz; La, Pr, Nd, Sm, Eu, Gd, Tb, Dy, Ho, Er, Tm, Yb, Lu (Fig. 5c).

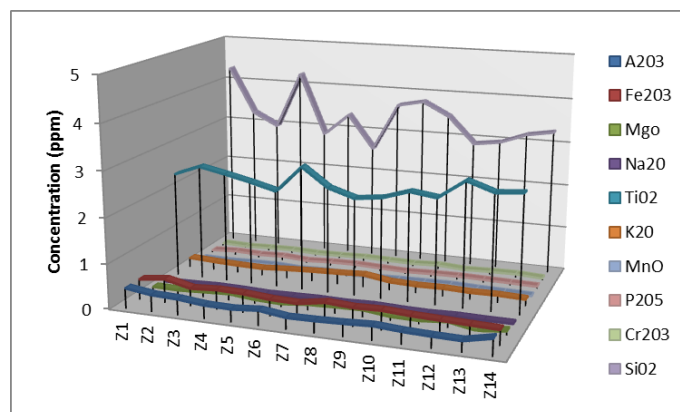


Figure 5a. Percentage composition of the major oxides in the studied samples

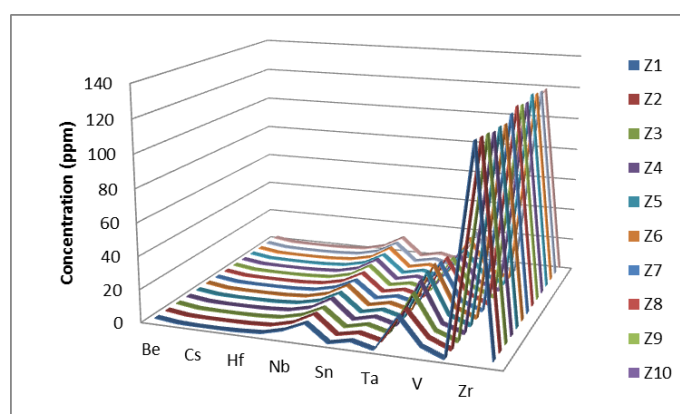


Figure 5b. Trace elements concentration in $\mu\text{g/g}$ (ppm)

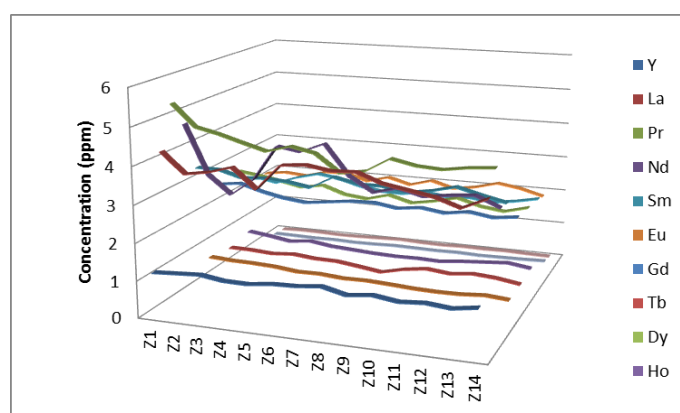


Figure 5c. Rare elements concentration in $\mu\text{g/g}$ (ppm)

The key indices (elements/oxides and oxide ratios) used for the chemostratigraphic zonation are: Zirconium (Zr) – to reveal the rate of terrigenous supply, Phosphorous (V) oxide (P_2O_5) – to ascertain the rate of biogenic productivity, Uranium (U) to determine the total of organic content, and Th/U ratio to contrast the quantity of clastic input with organic content of the rock samples. The chemostratigraphic subdivision of the study interval is shown in Fig. 6.

Surface geology of the study area was chemo-stratigraphically divided into two geochemical packages based on the observed contrast in the geochemical (log) signature of the area (Fig. 6). Package one and two were further subdivided into three and two units respectively.

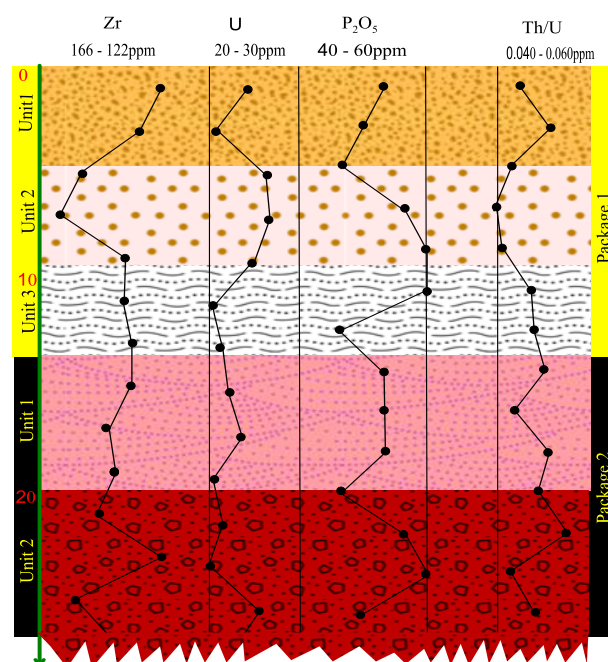


Figure 6. Chemostratigraphic zonation scheme of Lokoja-Bassange sedimentary outcrop

4.3 Package 1

This package depicts a drastic decrease in Zr but increased appreciably in the middle, maintaining an approximate steadiness to its base. The uranium content markedly decreased from top but almost immediately rebounded significantly to the middle portion of the log, and from this point, dropped drastically to the basal of the package. P_2O_5 is characterized by a gradual drop at the top, a continuous stretch of increase across the greater part of the package but with sharp drop at the base. The Th/U ratio log entirely exhibits a complete reversal of the U signature.

Unit 1: Terrigenous supply and clastic supply biogenic productivity steadily decrease within this unit. The organic content decreased to the mid of the unit, from where an increase was initiated to its base, but vice-versa for the clastic input.

Unit 2: The quantity of terrigenous supply and clastic input to the organic ratio both decreased abruptly; total organic content and bio-productivity contrarily increased remarkably in this unit. Supply, organic content, biogenic activities and a reduction in clastic input versus organic input.

Unit 3: Characterized by steady terrigenous supply; reduced organic content and biogenic activities and a minor increase in clastic input versus organic input.

4.4 Package 2

There is a perceptible semblance between Zr and P_2O_5 in the second package; both exhibiting steadiness from the top, slight decrement in the middle of the log, sharp increase further downward, and drastic reduction at the base. The uranium log is uniquely branded by a gradual rise from the top, slight reduction across the mid-section, and then a gentle at the base. However, the Th/U log fluctuates all through the length of the package.

Unit 1: Terrigenous mats, organic content and biogenic productivity were relatively stable in spite of the slight drop at the insignificant drop at the base of the unit. Fluctuations in clastic input - organic ratio occurred throughout the unit.

Unit 2: It is marked by a sharp increase, followed by a decrease in terrigenous mats, decrease in organic content, sporadic in increase in biogenic productivity, and a fluctuating clastic input versus organic input.

4.5 Facies changes

Table 3 interprets and identifies the sandstone facies in the study area based on the abundance of SiO_2/Al_2O_3 ratio, MgO and Fe_2O_3 of the analyzed sample. On the basis above interpretation, the facies change was modelled accurately (Fig. 7).

Table 3. Sandstone facies inferred in the study area (modified from [12])

Sample No	SiO_2/Al_2O_3	Fe_2O_3	MgO	Inference
1	9.56	5.69	1.12	Argillaceous sandstone
2	8.78	7.33	1.12	Argillaceous sandstone
3	8.45	5.86	1.66	Argillaceous sandstone
4	14.66	5.45	1.79	Sandstone
5	10.17	6.72	1.31	Sandstone
6	10.15	4.94	0.82	Sandstone
7	10.32	5.65	1.96	Sandstone
8	14.08	6.21	1.96	Sandstone
9	13.5	5.61	2.079	Sandstone
10	11.23	5.95	1.12	Sandstone
11	10.67	6.09	1.1	Sandstone
12	11.84	5.36	1.76	Sandstone
13	13.25	5.16	0.14	Sandstone
14	8.86	4.72	1.15	Argillaceous sandstone

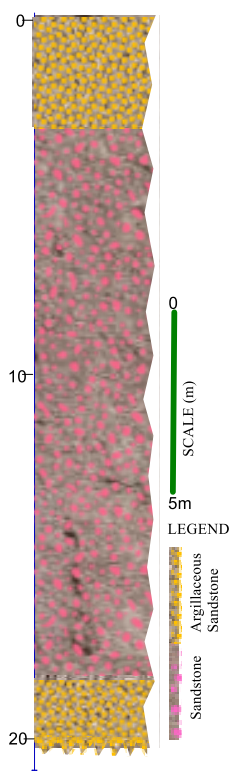


Figure 7. *Litho-section of surface samples*

4.6 Mineralogical interpretation of lithologic ratios

The Al_2O_3 content in the sample is apparently lower than that of the basic oxide ($\text{MgO} + \text{CaO} + \text{Na}_2\text{O} + \text{K}_2\text{O}$) in the investigated samples (Fig. 8), indicating very minimal degree of hydrolytic weathering of sourced grits.

Average $\text{Al}_2\text{O}_3/\text{SiO}_2$ value of **0.09** (Fig. 9a) in the samples indicates quartz enrichment [14]; but the complementary high average ratio of $\text{SiO}_2/\text{Al}_2\text{O}_3$ (**11.12**) can be inferred as an indicator of the intense chemical weathering. Derivation of source materials largely originated from a silica rich granitic source under a prolonged exposure to humid tropical condition. The Ga/Rb ratio ranges between 0.1 and 0.24 is typical of illinitic clay; inferentially indicative of exposure of argillaceous sandstone to a relatively cooler, drier condition during and after deposition. The binary plot of Ga and Rb is depicted below (Fig. 9b).

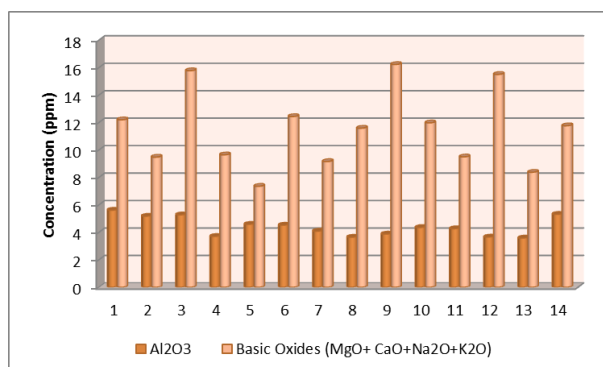


Figure 8. *Concentration of Al_2O_3 and bases in the sandstone samples*

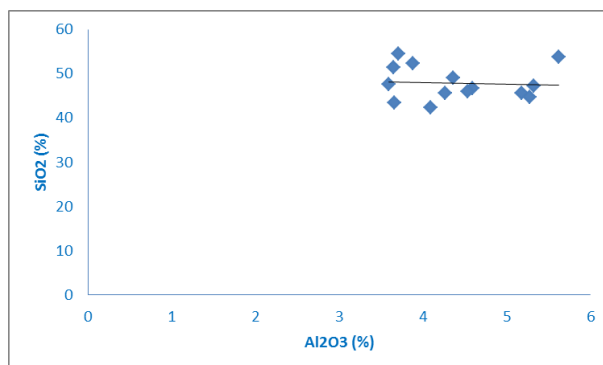


Figure 9a. Negative correlation chart of SiO_2 against Al_2O_3

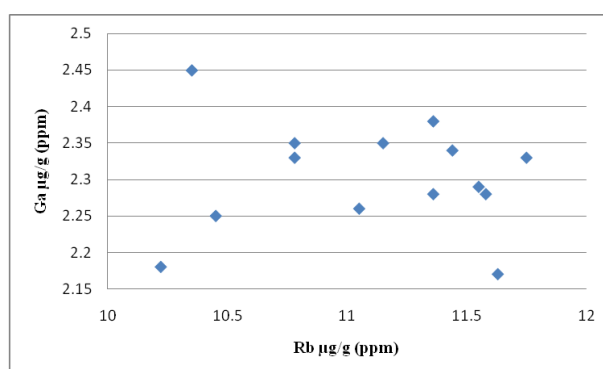


Figure 9b. Binary plot of Ga versus Rb

Ga/Rb ratio – Al_2O_3 /bases ratio discrimination plot (Fig. 9c) further affirmed the minimal degree of weathering of the sedimentary grits. Th/U ratio of the study samples range from 0.0391 and 0.0632 with an average of 0.0505; indicating minimal weathering of the source area or sediment recycling; this value-range is traditionally associated with active continental margin settings where rapid accumulation and burial of sediments can greatly occur. Also, these samples contain far greater proportions of Zircon (Fig. 9d) than Rutile and Anatase; and thus fall within the quartzite sedimentary rock. The periodic decrease and increase of Na_2O content in samples (Fig. 13) rather suggest differential preservation of plagioclase content, which can be closely linked with variations in chemical weathering intensity.

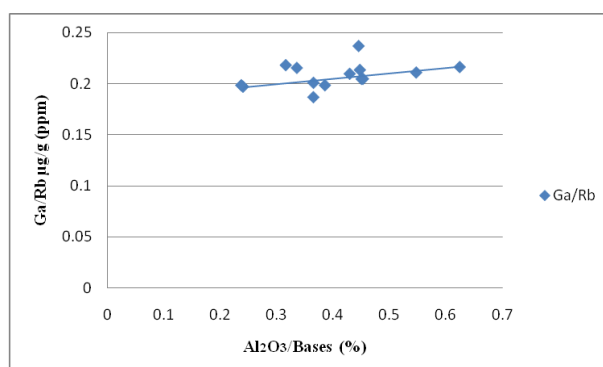


Figure 9c. Positive correlation plot of Al_2O_3 /bases versus Ga/Rb

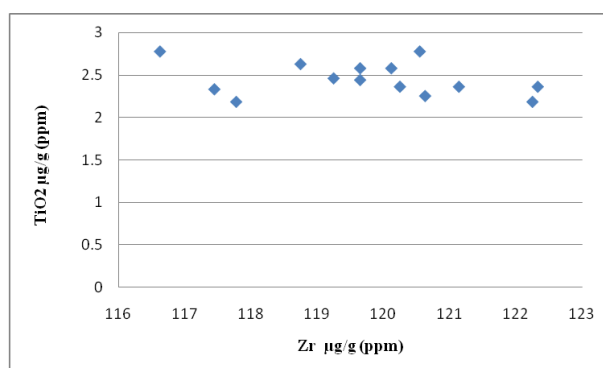


Figure 9d. Binary plot of TiO_2 against Zr

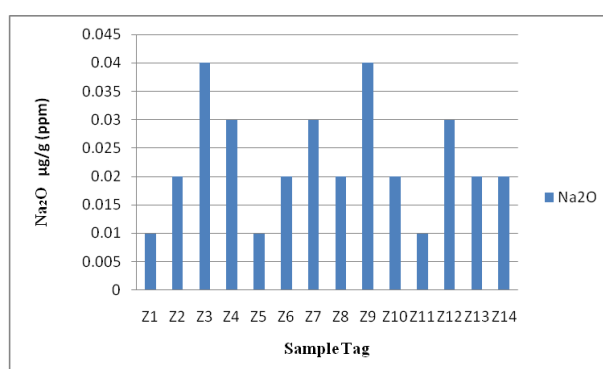


Figure 13. Na_2O content of Lokoja-Bassange formation through time

4.7 Provenance studies

Bulk of the sediments occupying the Campanian Lokoja-Bassange sandstone was more predictably sourced mainly from a quartzose sedimentary provenance (Fig. 14) which is an apparent indication of a reworked polycyclic sediment marked by several episodes of sedimentation (weathering, gravity, erosion, transportation, deposition and diagenesis) with minor augmentation from an igneous province within an active margin (Fig 15). Maturity is anticipated because of the prolonged transportation history of the sediments during this repetitive depositional cycle.

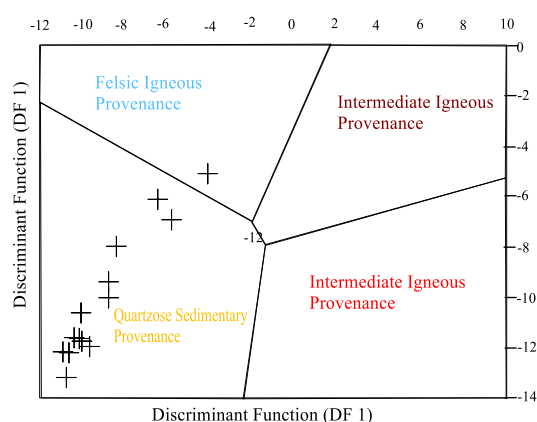


Figure 14. Discriminant provenance chart of the studied sandstones (modified from [20])

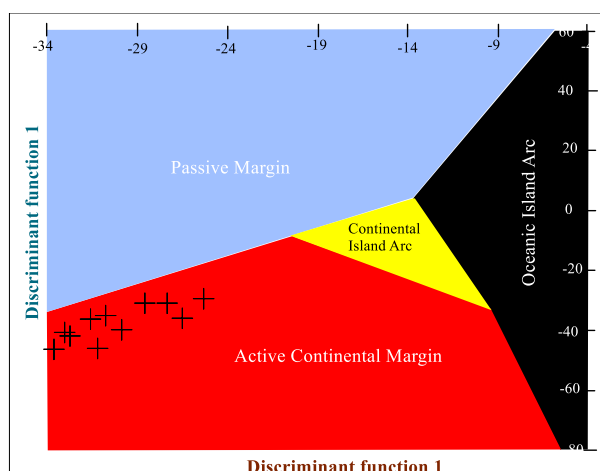


Figure 15. Discriminant tectonic chart study area (modified from [14])

CONCLUSION

Interpretation of whole rock geochemical data from the investigated sandstones delineated the uniqueness of geochemical signature of the various lithostratigraphic unit. Lokoja-Bassange formation contains single chemostratigraphic surfaces that can be approximated to a chronostratigraphic marker. Two chemostratigraphic packages and 5 units were identified and correlated. The formation was deposited and diagenized under a drier and cooler climate which evidently resulted in the relative abundance of illite in the argillaceous facies, while the older parts of the formation contain minor proportions of plagioclase feldspar, indicative of an igneous origin. Enrichment of Zr in the sandstone sample, reflects a heavy mineral (zircon) addition of a quartzose sedimentary provenance. The discriminant plots depict the derivation of the bulk of the sediment from a quartzose sedimentary provenance with minor relatively lesser supply from an igneous environment in an active continental setting.

REFERENCES

- [1] DAS, N. Chemostratigraphy of sedimentary sequences: A review of the state of the art. *Journal of the Geological Society of India*. 1997, vol. 49(6), pp. 621–628. ISSN 0016-7622. Available at: <http://www.geosocindia.org/index.php/jgsi/article/view/68709>
- [2] IKHANE, P.R., A.I. AKINTOLA, S.I. BANKOLE, O.M. AJIBADE and O.O. EDWARD. Chemostratigraphic Characterization of Siliciclastic Rocks in Parts of the Eastern Dahomey Basin, Southwestern Nigeria. *Journal of Geography and Geology*. 2014, vol. 6(4), pp. 88–108. ISSN 1916-9779. DOI: [10.5539/jgg.v6n4p88](https://doi.org/10.5539/jgg.v6n4p88)
- [3] SALUFU, S.O. and T.F. OGUNKUNLE T.F. Source Rock Assessment and Hydrocarbon Prospects of Anambra Basin: Salient Indications of Maturity. *Pacific Journal of Science and Technology*. 2015, vol. 16(1), pp. 336–344. ISSN 1551-7624. Available at: https://www.akamai.university/files/theme/AkamaiJournal/PJST16_1_336.pdf
- [4] REYMENT, R.A. *Aspect of the Geology of Nigeria: The Stratigraphy of the Cretaceous and Cenozoic Deposits*. Ibadan, Nigeria: Ibadan University Press, 1965.
- [5] OBI, G.C., C.O. OKOGBUE and C.S. NWAJIDE. Evolution of the Enugu Cuesta: A tectonically driven erosional process. *Global Journal of Pure and Applied Sciences*. 2001, vol. 7(2), pp. 321–330. ISSN 1118-0579. DOI: [10.4314/gjpas.v7i2.16251](https://doi.org/10.4314/gjpas.v7i2.16251)
- [6] BRUME, O. *Independent Geologic Field Mapping Report of the Igarra Axis of the Basement Complex and Benin Flanks of Anambra Basin in Northern Part of Edo State*. Unpublished field report. Effurun: Federal University of Petroleum Resources Effurun, 2014.

- [7] LADIPO, K.O. Paleogeography, sedimentation and tectonics of the upper cretaceous Anambra basin, southeastern Nigeria. *Journal of African Earth Sciences*. 1988, vol. 7(5–6), pp. 865–871. ISSN 0899-5362. DOI: [10.1016/0899-5362\(88\)90029-2](https://doi.org/10.1016/0899-5362(88)90029-2)
- [8] AKANDE, S.O., A. HOFFKNECHT and B.D. ERDTMANN. Upper Cretaceous and Tertiary Coals from Southern Nigeria: Composition, Rank, Depositional Environments and Their Technological Properties. *NAPE Bulletin*. 1992, vol. 7(1), pp. 26–38. ISSN 0794-0172.
- [9] PEARCE, T.J., D. WRAY, K. RATCLIFFE, D.K. WRIGHT and A. MOSCARIELLO. (2005a). Chemostratigraphy of the Upper Carboniferous Schooner Formation, southern North Sea. *Carboniferous hydrocarbon geology: the southern North Sea and surrounding onshore areas*. 2005, vol. 7, pp. 147–164. Available at: <http://www.k2sistemas.com.br/estratigrafiaquimica/artigos/2005/completo.pdf>
- [10] RATCLIFFE, K.T., J. MARTIN, T.J. PEARCE, A.D. HUGHES, D.E. LAWTON, D.S. WRAY and F. BESSA. A regional chemostratigraphically-defined correlation framework for the late Triassic TAG-I Formation in Blocks 402 and 405a, Algeria. *Petroleum Geoscience*. 2006, vol. 12(1), pp. 3–12. ISSN 1354-0793. DOI: [10.1144/1354-079305-669](https://doi.org/10.1144/1354-079305-669)
- [11] RATCLIFFE, K., M. WRIGHT, P. MONTGOMERY, A. PALFREY, A. VONK, J. VERMEULEN and M. BARRETT. Application of chemostratigraphy to the Mungaroo Formation, the Gorgon field, offshore northwest Australia. *The APPEA Journal*. 2010, vol. 50(1), pp. 371–388. ISSN: 2206-8996. DOI: [10.1071/AJ09022](https://doi.org/10.1071/AJ09022)
- [12] SPRAGUE, R.A., J.A. MELVIN, F.G. CONRADI, T.J. PEARCE, M.A. DIX, S.D. HILL and A. CANHAM. Integration of Core-based Chemostratigraphy and Petrography of the Devonian Jauf Sandstones, Uthmaniyah Area, Ghawar Field, Eastern Saudi Arabia. In: *AAPG Annual Convention: April 20–23, 2008, San Antonio, Texas*. AAPG, 2009. Available at: https://www.searchanddiscovery.com/documents/2009/20065sprague/ndx_sprague.pdf
- [13] RETALLACK, G.J. *A Colour Guide to Palaeosols*. Chichester, England: Wiley, 1997. ISBN 978-0471967118.
- [14] BHATIA, M.R. Plate Tectonics and Geochemical Composition of Sandstones. *Journal of Geology*. 1983, vol. 91(6), pp. 611–627. ISSN 0022-1376. DOI: [10.1086/628815](https://doi.org/10.1086/628815)
- [15] HIERONYMUS, B., B. KOTSCHOUBEY and J. BOULÈGUE. Gallium behaviour in some contrasting lateritic profiles from Cameroon and Brazil. *Journal of Geochemical Exploration*. 2001, vol. 72(2), pp. 147–163. ISSN 0375-6742. DOI: [10.1016/S0375-6742\(01\)00160-1](https://doi.org/10.1016/S0375-6742(01)00160-1)
- [16] WELBY, C.W. Occurrence of alkali metals in some Gulf of Mexico sediments. *Journal of Sedimentary Research*. 1958, vol. 28(4), pp. 431–452. DOI: [10.1306/74D70830-2B21-11D7-8648000102C1865D](https://doi.org/10.1306/74D70830-2B21-11D7-8648000102C1865D)
- [17] MCLENNAN, S.M., S. HEMMING, D.K. MCDANIEL and G.N. HANSON. Geochemical approaches to sedimentation, provenance and tectonics. *Special Papers of the Geological Society of America*. 1993, vol. 284, pp. 21–40. ISSN 0072-1077. DOI: [10.1130/SPE284-p21](https://doi.org/10.1130/SPE284-p21)
- [18] HILDRED, G.V., K.T. RATCLIFFE, A.M. WRIGHT, B.A. ZAITLIN and D.S. WRAY. Chemostratigraphic applications to low-accommodation fluvial incised-valley settings: An example from the Lower Mannville Formation of Alberta, Canada. *Journal of Sedimentary Research*. 2010, vol. 80(11–12), pp. 1032–1045. ISSN 1527-1404. DOI: [10.2110/jsr.2010.089](https://doi.org/10.2110/jsr.2010.089)
- [19] ROSER, B.P. and R.J. KORSCH. Determination of Tectonic Setting of Sandstone-Mudstone Suites Using SiO₂ Content and K₂O/Na₂O Ratio. *Journal of Geology*. 1986, vol. 94(5), pp. 635–650. ISSN 0022-1376. DOI: [10.1086/629071](https://doi.org/10.1086/629071)
- [20] ROSER, B.P. and R.J. KORSCH. Provenance signatures of sandstone-mudstone suites determined using discriminant function analysis of major element data. *Chemical Geology*. 1988, vol. 67(1–2), pp. 119–139. ISSN 0009-2541. DOI: [10.1016/0009-2541\(88\)90010-1](https://doi.org/10.1016/0009-2541(88)90010-1)